

## Si-Al order in leucite revisited: New information from an analcite-derived analogue

SIMON C. KOHN\*

Department of Physics, University of Warwick, Coventry CV4 7AL, U.K.

C. MICHAEL B. HENDERSON

Department of Geology, University of Manchester, Manchester M13 9PL, U.K.

RAY DUPREE

Department of Physics, University of Warwick, Coventry CV4 7AL, U.K.

### ABSTRACT

The Si-Al ordering in two contrasting samples of leucite was studied using MAS NMR. One sample was synthesized by performing an ion exchange, in molten KCl, on a natural analcite specimen that had a small distribution of Al next-nearest neighbors (NNN). The other leucite sample was a typical natural specimen from the Alban Hills. In the specimen derived by ion exchange, 45–50% of the Al is on T2 sites with the remainder distributed approximately equally between the T1 and T3 sites. The  $^{29}\text{Si}$  peak positions in this sample resolve a debate in the literature over assignment of the more complex  $^{29}\text{Si}$  spectra of natural leucite specimens. It is possible to simulate the  $^{29}\text{Si}$  spectrum of Alban Hills leucite with a wide variety of Al distributions, including either Al ordering onto T2 or Al ordering onto T1 + T3. By analogy with the analcite-derived sample and considering previous neutron and X-ray data, Al ordering onto T2 is considered somewhat more probable than the alternative schemes.

Site-ordering information obtained from  $^{27}\text{Al}$  NMR in an earlier study is not considered reliable because of complications arising from the differing (and uncertain) electric-field gradients at these sites.

### INTRODUCTION

At room temperature, the structure of leucite ( $\text{KAlSi}_2\text{O}_6$ ) is based on a three-dimensional interconnected tetrahedral framework with three crystallographically distinct tetrahedral sites (Mazzi et al., 1976). The role of ordering of Si and Al over these three sites in the structural phase transitions that occur at elevated temperatures has recently been the subject of debate. Hatch et al. (1990) suggested that Si-Al ordering was the driving force for the cubic-tetragonal phase transition, whereas Palmer and Salje (1990) favored a displacive mechanism that would not involve any Si-Al ordering. Recent lattice-energy calculations (Dove et al., 1993) also suggest that Si-Al ordering does not play an important role in triggering the transitions. Part of the reason for the continuation of this discussion is the lack of conclusive measurements of Si-Al ordering in the leucite phases. Early X-ray diffraction data suggested that Si and Al were completely disordered over the tetrahedral sites in both tetragonal and cubic phases (Peacor, 1968; Mazzi et al., 1976), and differences in heat capacity between data leucite and its Fe-bearing analogue,  $\text{KFeSi}_2\text{O}_6$ , were interpreted as being consistent with complete Si-Al disorder in both  $\text{KAlSi}_2\text{O}_6$

leucite symmetries (Lange et al., 1986). In contrast, Boyesen (1990) used neutron diffraction data to suggest that in the low-temperature  $I4_1/a$  phase Al is partially ordered onto T2 sites, implying a change in Si-Al order with increasing temperature.

NMR has been used to study structure and ordering in synthetic, Al-free leucite analogues (Kohn et al., 1991, 1994) and is, in principle, an ideal method for quantifying Si-Al ordering. However, the three published NMR studies of leucite (Brown et al., 1987; Murdoch et al., 1988; Phillips et al., 1989) reached opposing conclusions. The problem is that the  $^{29}\text{Si}$  spectrum for natural leucite consists of a broad envelope of resonances. Because there are three T sites in the structure and each Si can have zero, one, two, three, or four Al next-nearest neighbors (NNN), there are 15 possible Si environments. Thus, extraction of the required ordering information from the spectrum involves simulation of the lineshape with 15 lines of variable intensity, width, and position, i.e., 45 independent variables if no simplifying assumptions are made. Brown et al. (1987) used shifts calculated from the crystal structure to fit their spectrum and suggested that Al was preferentially ordered onto the T1 sites. In fact, their preferred Al occupancies of 0.56, 0.36, and 0.08 for T1, T2, and T3, respectively, imply noncompliance with Löwenstein's rule; the maximum Al occupancy consistent with Löwenstein behavior is (from the site connectivities) 0.50

\* Present address: Department of Geology, University of Bristol, Wills Memorial Building, Queens Road, Bristol BS8 1RJ, U.K.

for T1 and T3 and 1.00 for T2. The  $^{29}\text{Si}$  spectra in Murdoch et al. (1988) have a higher signal-to-noise ratio than those of Brown et al. (1987), and, by using more sophisticated fitting procedures, Murdoch et al. (1988) concluded that the Al occupancies of the three sites in natural leucite were 0.39 for T1, 0.16 for T2, and 0.42 for T3. Phillips et al. (1989) tried to avoid the difficulties of fitting a  $^{29}\text{Si}$  spectrum by concentrating on the  $^{27}\text{Al}$  spectrum of leucite. This approach has the advantage that only three Al lines can contribute to the spectrum (assuming Löwenstein behavior) but the disadvantage that the lines do not necessarily have simple Gaussian or Lorentzian shapes. Phillips et al. (1989) deduced Al occupancies of 0.50 for T1, 0.25 for T2, and 0.25 for T3. They suggested that the disagreement with the occupancies suggested by Murdoch et al. (1988) was due to incorrect assignment of the  $^{29}\text{Si}$  spectrum in the earlier study.

In the present study, a synthetic leucite has been prepared that has higher short-range order (i.e., a smaller distribution of Al NNN) and thus fewer, better resolved lines than the natural samples studied previously. The distribution of Al over the three tetrahedral sites, i.e., the long-range ordering, was determined using  $^{29}\text{Si}$  MAS NMR. By using the additional constraints provided by studying the synthetic sample, it was hoped that an improved measure of the Si-Al ordering in natural leucite would be obtained.

## EXPERIMENTAL METHODS

### Samples

The natural leucite sample, KAS2, is a specimen from the Alban Hills, in the Roman volcanic province, Italy. The synthetic leucite sample, KAS3, was made by ion exchange from a natural analcite sample, M416, from Montecchio, Maggiore, Italy. The ion exchange was performed by grinding the analcite into powder of less than about 20  $\mu\text{m}$  diameter and then refluxing the powder in molten KCl at 850  $^{\circ}\text{C}$  for two periods of 3 h in a Pt crucible. The natural minerals were analyzed by EPMA and found to have the compositions of  $\text{Na}_{1.00}\text{Al}_{0.99}\text{Si}_{2.01}\text{O}_6 \cdot \text{H}_2\text{O}$  and  $\text{K}_{0.94}\text{Na}_{0.02}\text{Fe}_{0.01}\text{Al}_{1.00}\text{Si}_{2.00}\text{O}_6$ , respectively. The composition of the leucite derived from ion exchange was checked by atomic absorption spectroscopy; the sample contained 309 ppm Na, indicating that the ion exchange had proceeded nearly to completion. Synchrotron X-ray powder diffraction patterns for M416 analcite show a shoulder on the high  $2\theta$  side of the 400 peak, suggesting that the sample is not cubic  $1a3d$  (cf. Mazzi and Galli, 1978). The pseudocubic ( $1a3d$ ) cell parameter obtained is 13.721  $\text{\AA}$ , whereas preliminary tetragonal ( $I4_1/acd$ ) parameters are  $a = 13.732$ ,  $c = 13.713$   $\text{\AA}$ . The cell parameters for the leucite samples are as follows: Alban Hills leucite (KAS2),  $a = 13.061$ ,  $c = 13.754$   $\text{\AA}$ ; leucite derived from analcite (KAS3),  $a = 13.037$ ,  $c = 13.740$   $\text{\AA}$ .

### NMR

The  $^{29}\text{Si}$  NMR data were acquired using a Bruker MSL 360 spectrometer (8.45 T) operating at 71.535 MHz with

MAS at 3.0–3.5 kHz. The spin-lattice relaxation time ( $T_1$ ) for the analcite-derived  $\text{KAlSi}_2\text{O}_6$  was extremely long (several hours), therefore it was difficult to obtain a spectrum with good signal-to-noise ratio. For analcite,  $^1\text{H}$ - $^{29}\text{Si}$  cross-polarization experiments were also used.

The  $^{27}\text{Al}$  spectra were obtained at two fields. The main experiments were performed using a Varian VXR 600 spectrometer (14.1 T). Use of the highest possible magnetic fields gives optimum resolution between the different Al sites because of the decrease in importance of quadrupolar broadening. Additional spectra were obtained on the MSL 360, principally to deduce the values of the quadrupole parameters for the three Al sites and hence to calculate their influence on the positions, shapes, and intensities of the peaks in the high-field spectra. It is possible, in principle, to obtain this information both from the changes in the central transitions between the two fields and from differences between the center band and the spinning sidebands of the satellite transitions at a given field (Jäger et al., 1992). In practice it was found that useful satellite transition spectra could be obtained only on the MSL 360 because of spinning speed instability on the VXR 600.

## RESULTS

### Analcite

The single-pulse  $^{29}\text{Si}$  spectrum for M416 analcite (Fig. 1a) consists of a peak at  $-96.6$  ppm with a small narrow feature at  $-91.5$  ppm and a small, broader feature at  $-102$  ppm. The main peak is clearly due to  $Q^4(2\text{Al})$  Si, and, as the small peaks are around 5 ppm away from the main peak, the  $-91.5$  ppm peak is due to  $Q^4(3\text{Al})$  and the  $-102$  ppm peak to  $Q^4(1\text{Al})$  Si. In cross-polarization spectra (Fig. 1b) where  $^1\text{H}$ -decoupling was also used, the peaks were slightly narrower, but no significant changes in the relative intensities of the three peaks were observed. The Si atoms in this analcite specimen have a much smaller distribution in the numbers of Al NNN than other analcite samples studied previously in this laboratory or in the literature (Fyfe et al., 1983; Murdoch et al., 1988). For example, in the analcite spectrum reported by Fyfe et al. (1983) five  $^{29}\text{Si}$  peaks are present, corresponding to zero, one, two, three, and four Al NNN. Preliminary X-ray investigations (S.A.T. Redfern, personal communication; A.M.T. Bell et al., personal communication) suggest that M416 analcite is noncubic, implying that there are two or three crystallographically distinct sites (Mazzi and Galli, 1978). This would be consistent with the NMR data only if the sites were too similar to each other in terms of Si-O distance, Si-O-Si angle, etc., to be resolved.

Generally the relative intensities of peaks in  $^1\text{H}$  to  $^{29}\text{Si}$  cross-polarization spectra are not representative of the concentrations of Si in the different sites. However, in this case we chose to simulate the cross-polarization spectrum with the longest contact time (20 ms) because: (1) the cross-polarization and single-pulse spectra clearly have

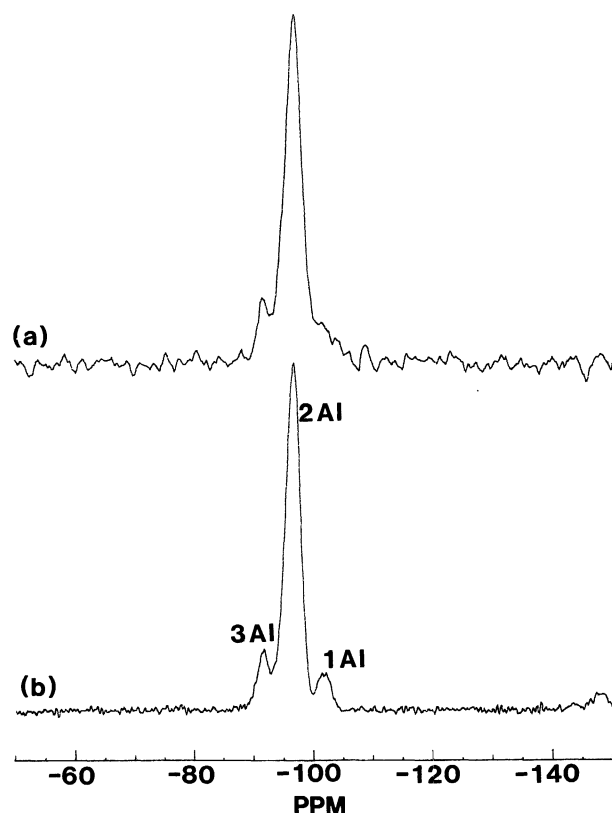


Fig. 1. The  $^{29}\text{Si}$  spectra of analcite. (a) Single-pulse spectrum acquired using  $104\ 2\ \mu\text{s}$  ( $\pi/6$ ) pulses, with a 30 s recycle delay. (b) Cross-polarization spectrum for a contact time of 20 ms; 600 FIDs were acquired with a 10 s recycle delay.

very similar relative areas for the three peaks; (2) the relative areas are rather insensitive to contact time between 0.5 and 20 ms; (3) it has a much higher signal-to-noise ratio than the single-pulse spectrum; and (4) the peaks are better resolved, presumably because of the removal of residual dipolar coupling between  $^1\text{H}$  and  $^{29}\text{Si}$ . The relative areas of the 3Al, 2Al, and 1Al peaks are 12.3, 80.5, and 7.2, respectively; the Si-Al ratio was calculated using the method of Klinowski et al. (1982) and found to be  $1.97 \pm 0.05$ . This is close to the value of  $2.03 \pm 0.06$  from EPMA and indicates that, as expected, Löwenstein's rule is obeyed.

The  $^{27}\text{Al}$  spectrum of analcite obtained at 14.1 T (156.3 MHz) consists of a single peak at 57.9 ppm with a FWHM of 2.5 ppm, consistent with the presence of either a single tetrahedral site or two or three sites with very similar local geometries. One would expect only one Al peak per T site, as any additional peaks would indicate departure from Löwenstein behavior.

#### Analcite-derived leucite

The  $^{29}\text{Si}$  spectrum of leucite obtained by ion exchange from analcite (KAS3) has three main peaks and some smaller features (Fig. 2a). It was difficult to obtain a spectrum with a high signal-to-noise ratio because of the ex-

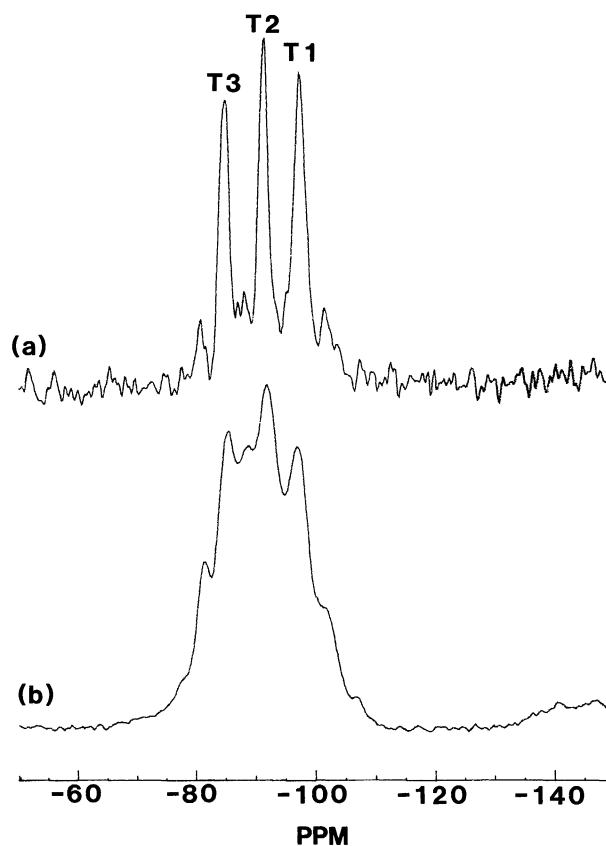
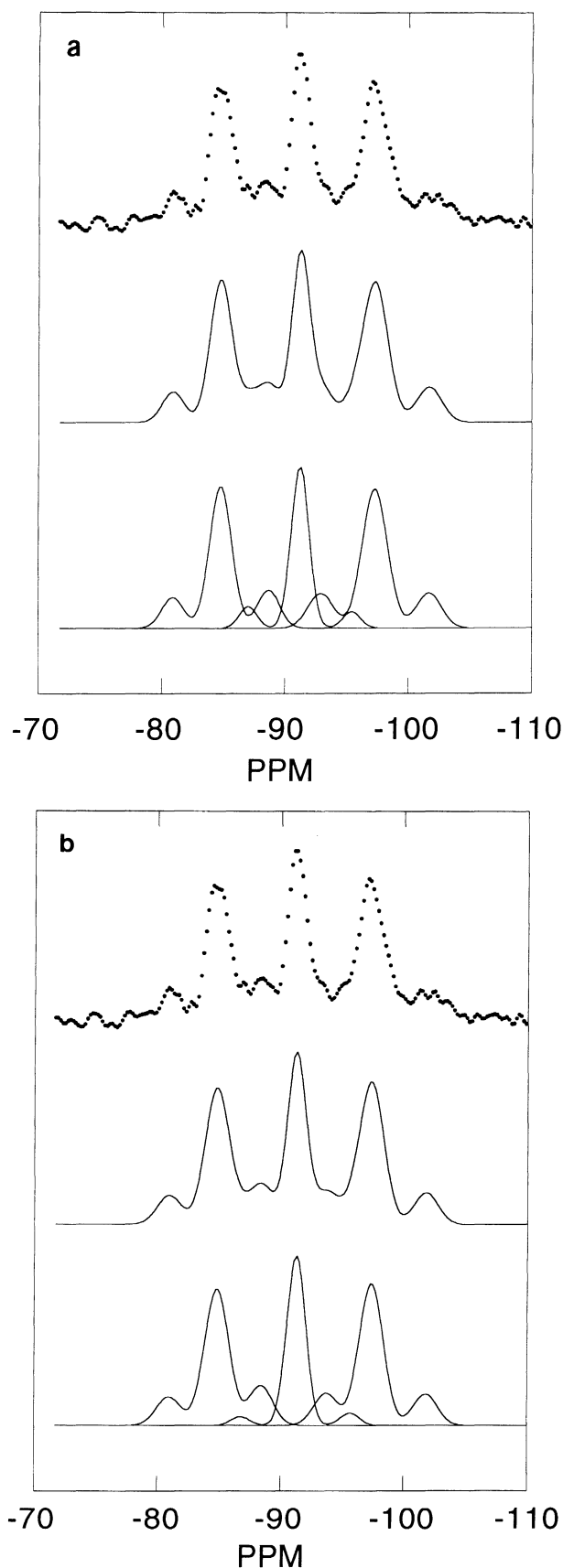


Fig. 2. The  $^{29}\text{Si}$  spectra of leucite. (a) KAS3 leucite derived by ion exchange from analcite. The spectrum shown is the result of the addition of three spectra all acquired using a  $2\ \mu\text{s}$  pulse length: (1) 84 pulses, 30 min recycle delay; (2) 32 pulses, 120 min recycle delay; (3) 48 pulses, 60 min recycle delay. The total acquisition time for this spectrum was 154 h; (b) KAS2 natural Alban Hills leucite; 4000 pulses, with a 1 s recycle delay.

tremely long spin-lattice relaxation time, therefore the spectrum shown in Figure 2a was obtained by adding several spectra with different recycle delays. By analogy with the analcite starting material (see above), and assuming that the distribution of Al NNN does not change significantly during the ion exchange, the three main peaks at  $-97.3$ ,  $-91.3$ , and  $-84.8$  ppm can be assigned to  $Q^4(2\text{Al})$  Si atoms on the T1, T2, and T3 sites, respectively. These chemical shifts are quite close to the values of  $-98.1$ ,  $-92.9$ , and  $-85.2$ , respectively, calculated from the crystal structure by Murdoch et al. (1988) using the method of Ramdas and Klinowski (1984). It can be seen from a superficial examination of the spectrum that the intensities of the three main peaks are similar, although the T2 peak is somewhat narrower, suggesting that it has the smallest area. More detailed information on Si-Al ordering was obtained by performing computer simulations. Given the signal-to-noise ratio of the spectrum, it was unrealistic to let all the possible parameters vary during the simulation or to try to use all 15 of the possible peaks. Therefore, three assumptions were made: (1) only



**TABLE 1.** Results of simulation of the  $^{29}\text{Si}$  spectrum of KAS3, the leucite derived by ion exchange from analcite, assuming constant FWHM and  $\Delta\delta$  within each group

Site	$n^*$	$\delta$	FWHM	Area**
T3	3	-80.90	2.1	4.3
T3	2	-84.80	2.1	23.1
T3	1	-88.70	2.1	6.1
T2	3	-87.05	1.7	2.4
T2	2	-91.25	1.7	21.3
T2	1	-95.45	1.7	2.1
T1	3	-92.90	2.4	6.2
T1	2	-97.30	2.4	27.7
T1	1	-101.70	2.4	6.9

Note: these parameters give the best numerical fit but do not include internal consistency considerations. All lines are Gaussian in shape.

\* Number of Al next-nearest neighbors for the Si, i.e.,  $Q^n(n\text{Al})$ .

\*\* Area of each peak expressed as a percentage of the total spectrum area. The figures given are the means of the fits to two  $^{29}\text{Si}$  spectra of KAS3.

nine possible peaks, i.e., those due to  $Q^1(1\text{Al})$ ,  $Q^2(2\text{Al})$ , and  $Q^3(3\text{Al})$  for each of the three T sites, have significant intensity (on the basis of Al NNN distribution in the parent analcite); (2) the peaks are all Gaussian in shape; (3) within each group (i.e., T1, T2, and T3) the widths of the three peaks are due to one, two, and three Al NNN are fixed.

It is possible to simulate the spectra in two entirely different ways. Either the best purely numerical fit is found, or internal consistency is included. The check on internal consistency results from the fact that the mean number of Al NNN around the Si in each site can be calculated using two independent methods. First, for each site, the mean number of Al NNN is equal to the sum of each  $n\text{Al}$  peak multiplied by  $n$ , this sum then being divided by the total Si occupancy,  $[\sum_{\delta} nI(n\text{Al})]/[\sum_{\delta} I(n\text{Al})]$ . The second method of calculating the mean number of Al NNN around the Si in each site uses the T-site occupancies. Let the Al occupancies of the T1, T2, and T3 sites be  $\alpha$ ,  $\beta$ , and  $\gamma$ , respectively, and consider the case of a Si atom on the T1 site. On average, each T1 site contains  $\alpha$  Al and  $(1 - \alpha)$  Si. Each T1 site is surrounded by two T1 sites and two T2 sites; therefore there are  $(2\alpha + 2\beta)$  Al and  $(4 - 2\alpha - 2\beta)$  Si in the NNN shell. But, if Löwenstein's rule is obeyed, the Al atoms on T1 are all surrounded by four Si atoms; therefore,  $4\alpha$  Si is effectively removed from the NNN shell of Si, and the NNN shell of a Si on the T1 site is  $(2\alpha + 2\beta)$  Al and  $(4 - 6\alpha - 2\beta)$  Si.

Although one might expect that the two simulations would give the same result, we find that for both KAS3

←

Fig. 3. Examples of simulations of  $^{29}\text{Si}$  spectrum of leucite derived by ion exchange, KAS3. (a) Best numerical fit but not forcing internal consistency (upper) experimental data (sum of two experiments, 84 pulses with a 30 min recycle delay and 32 pulses with a 120 min recycle delay). (middle) Simulation of the spectrum with the nine peaks listed in Table 1. (lower) The three sets of peaks for the three T sites. (b) As a but including internal consistency constraint. The positions, widths, and intensities of the nine peaks are given in Table 2.

**TABLE 2.** Results of simulation of the  $^{29}\text{Si}$  spectrum of KAS3, the leucite derived by ion exchange from analcite, with internal consistency constraint

Site	$n^*$	$\delta$	FWHM	Area**
T3	3	-80.95	2.3	5.1
T3	2	-84.83	2.3	24.4
T3	1	-88.43	2.3	7.1
T2	3	-86.80	1.8	1.2
T2	2	-91.29	1.8	23.7
T2	1	-95.70	1.8	1.8
T1	3	-93.72	2.3	5.8
T1	2	-97.38	2.3	25.3
T1	1	-101.80	2.3	5.6

Note: parameters modified from those in Table 1 by relaxing the constraint of constant  $\Delta\delta$  within each group. All lines are Gaussian in shape.

\* Number of Al next-nearest neighbors for the Si, i.e.,  $Q^*(n\text{Al})$ .

\*\* Area of each peak expressed as a percentage of the total spectrum area. The figures given are for the  $^{29}\text{Si}$  spectrum of KAS3 with the better signal-to-noise ratio.

and KAS2 this is not the case. We therefore present two simulations for each sample and discuss the implications of any differences between them.

The best numerical fit to the spectrum of KAS3 was obtained by fixing the widths of the T1, T2, and T3 peaks at 2.4, 1.7, and 2.1 ppm, respectively (these values were chosen on the basis of a preliminary three-peak simulation), and assuming that the difference in shift between  $n = 1$  and  $n = 2$  is the same as the difference in shift between  $n = 2$  and  $n = 3$  for each of the three groups. The best fit was obtained if the shift changes per Al substitution were set at 4.4, 4.2, and 3.9 ppm for the T1, T2, and T3 peaks, respectively. This compares with values of  $5.0 \pm 0.3$ ,  $4.5 \pm 0.2$ , and  $4.25 \pm 0.1$  given by Murdoch et al. (1988, their Table 8), for natural and gel-synthesized leucite. Simulations of two independent spectra for KAS3 were performed to give some idea of the statistical errors involved, and the mean results of these simulations are given in Table 1. The simulation of one of the spectra is shown in Figure 3a. The simulated Si-Al ratio is  $2.02 \pm 0.04$ , consistent with the value for the analcite precursor, and the distribution of Si over the three T sites is  $40.8 \pm 2.0\%$  in T1,  $25.9 \pm 2.0\%$  in T2, and  $33.4 \pm 2.0\%$  in T3. These values yield Si occupancies of  $0.82 \pm 0.04$  for T1,  $0.52 \pm 0.04$  for T2, and  $0.67 \pm 0.04$  for T3. Converting these to Al occupancies,  $g_i$ , gives  $g_1 = 0.18 \pm 0.04$ ,  $g_2 = 0.48 \pm 0.04$ , and  $g_3 = 0.33 \pm 0.04$ .

The second method of simulation forces the data to be internally consistent but relaxes the assumption of fixed shifts per Al substitution on each site, i.e., all peak positions are allowed to vary. Since the Si-Al ratio is 2 and the majority of Si atoms have two Al NNN, the Si occupancies of the T1 and T3 sites must be equal. Thus, the total intensity of the T3 peaks was forced to be equal to the total intensity of the T1 peaks. The best example of a simulation of this type is shown in Figure 3b, and the parameters are listed in Table 2, although it should be noted that all fits that included internal consistency had a larger  $\chi^2$ . Al occupancies are  $g_1 = 0.27$ ,  $g_2 = 0.47$ , and  $g_3 = 0.27$ , and  $\langle n\text{Al} \rangle = 1.98 \pm 0.03$  for all three sites.

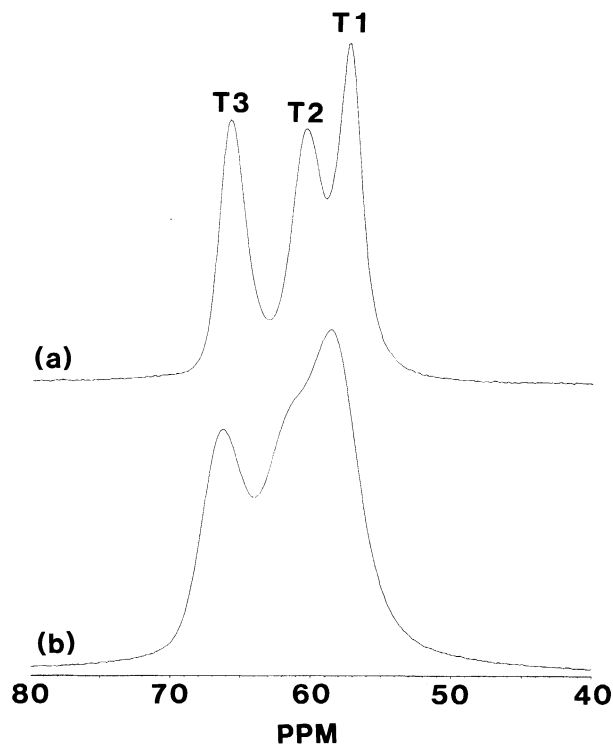


Fig. 4. The  $^{27}\text{Al}$  spectra of leucite obtained at a frequency of 156.3 MHz and using a  $1 \mu\text{s}$  ( $\pi/12$ ) pulse. (a) KAS3 leucite derived by ion exchange from analcite: 928 pulses, 1 s recycle delay; (b) KAS2 natural Alban Hills leucite: 2400 pulses, 0.1 s recycle delay.

These figures compare with  $g_1 = 0.39$ ,  $g_2 = 0.16$ , and  $g_3 = 0.42$  given in Murdoch et al. (1988). Thus, instead of Al deficiency on T2 as suggested by Murdoch et al. (1988) for a natural leucite, we observe an excess of Al on T2 in KAS3, and this is the case in all the simulations we performed. The fact that the fit with internal consistency does not give the best numerical fit may suggest that there is some nonrandom ordering in addition to Löwenstein behavior.

The high-field  $^{27}\text{Al}$  spectrum for the leucite derived by ion exchange (KAS3) (Fig. 4a) consists of three partially resolved peaks at around 57.5, 60.6, and 65.9 ppm due to T1, T2, and T3 sites. However, extraction of the peak areas, and hence the Al occupancies of the three T-sites, is far from straightforward. In contrast to  $^{29}\text{Si}$  spectra, the lineshapes in  $^{27}\text{Al}$  MAS spectra for an ideal, ordered system are generally not symmetrical because the resonances have the well-known second-order quadrupolar lineshapes (e.g., Kirkpatrick, 1988; Smith, 1993). In the absence of any resolvable second-order quadrupolar structure in the individual resonances, several different approaches are possible. Phillips et al. (1989) measured both the  $^{27}\text{Al}$  center band and the spinning sidebands of the satellite transitions to estimate the quadrupolar shift and the isotropic chemical shifts of the three resonances. However, in fitting their spectra they assumed that quadrupolar effects play a negligible role in determining the

lineshape and simulated their spectrum using mixed Gaussian and Lorentzian components. Although the parameters they deduced appeared to be internally consistent, they were careful to point out the possible errors that the assumption of symmetrical lineshapes could introduce.

Simulation of the  $^{27}\text{Al}$  spectrum of KAS3 using peak shapes with 60% Gaussian and 40% Lorentzian components gave peaks at 57.5 ppm (FWHM = 2.0 ppm), 60.6 ppm (FWHM = 2.8 ppm), and 65.9 ppm (FWHM = 2.3 ppm), corresponding to T1, T2, and T3 sites, respectively, with the Al distributed over the three T sites as follows:  $g_1 = 0.33$ ,  $g_2 = 0.35$ , and  $g_3 = 0.32$ . These figures are clearly in poor agreement with the values deduced by simulation of the  $^{29}\text{Si}$  spectrum; therefore it must be concluded that one or both simulations are in error. We do not consider it probable that the  $^{29}\text{Si}$  results could be so much in error, since we performed many simulations using different sets of assumptions, and in all cases the Si occupancy of the T2 site is the lowest, implying that the Al occupancy of the T2 site must be higher than that of the other two sites. It therefore appears that the simulation of the  $^{27}\text{Al}$  spectrum is unreliable. An important source of error is the assumption of simple mixed Gaussian and Lorentzian lines. The spectrum appears to be slightly skewed to more negative shifts, presumably because of quadrupolar effects producing a tail on the right side of the spectrum. This tail appears to be real, as the same feature has also been observed in the  $^{27}\text{Al}$  spectra of Rb- and Cs-exchanged leucite synthesized from the same analcite precursor (Kohn et al., in preparation). However, it should be noted that the  $^{27}\text{Al}$  peak for the T3 site is almost completely resolved from the T2 and T1 peaks, so the error in the area of the T3 peak as a fraction of the total area of the spectrum is probably relatively small and primarily due to the fitting of the T2 and T1 peaks. It is therefore encouraging to note that the values of  $g_3 = 0.32$  deduced from the  $^{27}\text{Al}$  spectrum and  $g_3 = 0.27$  or  $0.33$  from the  $^{29}\text{Si}$  spectra are, within error, the same.

To reconcile the  $^{29}\text{Si}$  and  $^{27}\text{Al}$  data in a more quantitative way, we also simulated the  $^{27}\text{Al}$  spectrum using dipolar-broadened quadrupolar lineshapes. Because we obtained  $^{27}\text{Al}$  spectra at two fields (14.1 and 8.45 T), the parameters used to fit the spectrum at one field can be checked by using them to simulate the spectrum at the other field. Furthermore, a first estimate of the quadrupole coupling constants for Al in the three sites can be obtained by measuring the quadrupolar shift between the center band and the spinning sidebands of the satellite transitions in the 8.45 T spectrum (Phillips et al., 1989; Jäger et al., 1992). This procedure gives values of the quadrupole coupling constant,  $C_q$ , in the range 1.3–2.0 MHz with T1 apparently having the smallest  $C_q$  (1.3 MHz). It is found that no set of parameters gives a satisfactory fit to both high- and low-field spectra, but that the broad features of both spectra were reproduced with the following set of parameters: T1:  $C_q = 1.3$  MHz;  $\eta =$

0.2;  $\delta_{\text{iso}} = 58.5$ ; dipolar broadening = 350 Hz; Al occupancy = 0.32. T2:  $C_q = 2.0$  MHz;  $\eta = 0.2$ ;  $\delta_{\text{iso}} = 62.5$ ; dipolar broadening = 500 Hz; Al occupancy = 0.37. T3:  $C_q = 1.7$  MHz;  $\eta = 0.2$ ;  $\delta_{\text{iso}} = 67.5$ ; dipolar broadening = 350 Hz; Al occupancy = 0.30, where  $\eta$  is the asymmetry parameter and  $\delta_{\text{iso}}$  is the isotropic chemical shift. Two additional sources of error in these simulations might account for the remaining discrepancies between the relative areas of the peaks in the simulations and the predictions (which we consider to be more reliable) from the fits of the  $^{29}\text{Si}$  spectrum. Probably the most important deficiency of the  $^{27}\text{Al}$  simulations is that they do not take into account any distribution in the quadrupole parameters. It was previously demonstrated that a distribution in  $C_q$  gives rise to an asymmetrical peak that is skewed to more negative shifts (Phillips et al., 1988). If the lineshapes have different degrees of asymmetry, the relative intensities could easily be changed to become consistent with the  $^{29}\text{Si}$  data. An additional factor that could play a role is a contribution to the intensities of the center bands from the  $^{27}\text{Al}$  satellite transitions, i.e.,  $1/2$  to  $3/2$  and  $3/2$  to  $5/2$  transitions. Generally, if  $C_q$  is fairly large the contribution of the satellite transitions is assumed to be negligible, but if  $C_q$  is small (as it is here) this assumption may not be valid. If  $C_q$  is smaller for T1 and T3 than for T2, as found above, then the T1 and T3 peaks will appear relatively enhanced. Although this reduces the calculated Al occupancies toward those obtained from the  $^{29}\text{Si}$  data, we calculate (using our estimates of the quadrupole coupling constants given above) that the differences between the contributions of the satellite transitions for the three sites are not large enough to be the principal cause of the disagreement between the  $^{29}\text{Si}$  and  $^{27}\text{Al}$  simulations.

One final point of interest in the data for KAS3 is that the amount of Si with other than two Al NNN appears to be somewhat different from the analcite precursor. Whereas the analcite has 20% of the Si with one or three Al NNN and 80% with two Al NNN, the leucite derived from it by ion exchange has  $27 \pm 1\%$  Si with one or three Al NNN. It therefore appears that there has been a small decrease in Al-Si order during the ion-exchange process. This is in contrast to the usual assumption that Al-Si ordering in framework silicates in general is far too slow to change on the timescale of the ion exchange (e.g., Hovis, 1986).

#### Alban Hills leucite

The  $^{29}\text{Si}$  spectrum for natural Alban Hills leucite, KAS2, is given in Figure 2b. It consists of a relatively broad resonance with eight discernible features (peaks or shoulders). This spectrum is very similar to those previously obtained by Brown et al. (1987), Murdoch et al. (1988), and Phillips et al. (1989), and it has been shown by these authors that this spectrum can be simulated by the superposition of 8–15 relatively narrow lines. The most intense features are at  $-96.8$ ,  $-91.6$ , and  $-85.3$  ppm, close to those for the three main peaks in  $\text{KAlSi}_2\text{O}_6$  (KAS3) derived by ion exchange, indicating that these features

**TABLE 3.** Results of a simulation of the  $^{29}\text{Si}$  spectrum of KAS2, the natural Alban Hills leucite, which gives an ordering scheme where Al is ordered onto the T2 site

Site	$n^*$	$\delta$	FWHM	Area**
T3	4	-77.20	2.8	2.5
T3	3	-81.10	2.8	8.0
T3	2	-85.00	2.8	14.3
T3	1	-88.90	2.8	9.8
T3	0	-92.80	2.8	2.3
T2	4	-82.85	2.7	2.0
T2	3	-87.05	2.7	4.9
T2	2	-91.25	2.7	8.4
T2	1	-95.45	2.7	5.7
T2	0	-99.65	2.7	2.2
T1	4	-88.00	3.3	2.7
T1	3	-92.70	3.3	12.0
T1	2	-97.40	3.3	15.2
T1	1	-102.10	3.3	7.6
T1	0	-106.80	3.3	2.3

Note: the peak positions were kept as close as possible to the positions deduced for KAS3, and FWHM and  $\Delta\delta$  within each group were forced to be constant but internal consistency was not considered. All lines are Gaussian in shape.

\* Number of Al next-nearest neighbor for the Si, i.e.,  $Q^4(n\text{Al})$ .

\*\* Area of each peak expressed as a percentage of the total spectrum area.

**TABLE 4.** Results of an alternative simulation of the  $^{29}\text{Si}$  spectrum of KAS2 (shown in Fig. 5), including internal consistency constraint and Al ordering onto the T2 site

Site	$n^*$	$\delta$	FWHM	Area**
T3	4	-77.20	2.8	2.5
T3	3	-81.10	2.8	8.0
T3	2	-85.00	2.8	14.3
T3	1	-88.90	2.8	8.0
T3	0	-92.80	2.8	2.5
T2	4	-82.93	3.0	2.1
T2	3	-87.33	2.8	6.2
T2	2	-91.29	3.0	11.6
T2	1	-95.08	3.5	7.9
T2	0	-99.80	2.3	1.9
T1	4	-88.00	3.3	2.3
T1	3	-92.70	3.3	7.6
T1	2	-97.40	3.3	15.2
T1	1	-102.10	3.3	7.6
T1	0	-106.80	3.3	2.3

Note: the T1 and T3 envelopes were assumed to be symmetrical and given fixed intensities, and all the parameters for the T2 peaks were allowed to vary. All lines are Gaussian in shape.

\* Number of Al next-nearest neighbors for the Si, i.e.,  $Q^4(n\text{Al})$ .

\*\* Area of each peak expressed as a percentage of the total spectrum area.

are due predominantly to  $Q^4(2\text{Al})$  Si atoms in T1, T2, and T3 sites, respectively. These assignments are in agreement with those of Murdoch et al. (1988) but not with those of Phillips et al. (1989), casting doubt on the Si-Al ordering scheme suggested by Phillips et al. (1989). Again, we simulated the spectrum in two ways. The first simulation represents the best numerical fit using starting assumptions similar to those used for KAS3 irrespective of internal consistency considerations. The  $Q^4(2\text{Al})$  peak positions and shifts per Al substitution for each T site were the same as those obtained in the unconstrained fit of KAS3, and the widths were forced to be the same within each set of five ( $n = 0-4$ ) peaks. The peak widths are broader than in the sample derived by ion exchange because of increased disorder in the fourth-nearest neighbor and more distant shells, increased distribution in the local geometries of the sites, or both factors. Minor adjustments to the positions of the sets of peaks and the spacing between peaks within a set improve the fit, and, in the best numerical fit we were able to obtain (Table 3), the  $Q^4(2\text{Al})$  shifts are -97.4, -91.25, and -85 ppm, i.e., more negative by 0.1 ppm for T1 and 0.2 ppm for T3 than in KAS3. The Si-Al ratio calculated from this fit is 1.98, in excellent agreement with the value of 2.00 from EPMA, and the distribution of Si over the three sites is 40% in T1, 23% in T2, and 37% in T3, corresponding to Al occupancies of  $g_1 = 0.20$ ,  $g_2 = 0.54$ , and  $g_3 = 0.26$  (equivalent to approximately one-half the Al occupying T2 sites and one-quarter occupying each of the T1 and T3 sites).

In the second fit to KAS2, we assumed symmetrical  $n\text{Al}$  envelopes for the T1 and T3 sites and allowed all the parameters for the T2 site to vary. This approach is based on the observation that the extreme high-field and low-

field portions of the spectrum are fairly well resolved. The widths of the T3 and T1 peaks are fixed at 2.8 and 3.3 ppm, respectively, and the peak positions are fixed to be the same as in the previous fit. The positions, widths, and intensities of the T2 peaks are all allowed to vary, resulting in widths of 2.3-3.5 ppm, interpeak spacings of 3.8-4.7 ppm, and a symmetrical envelope, all of which seem reasonable. The slightly narrow width (2.3 ppm) of the T2 (0Al) peak could be increased to make it more consistent with the other peaks (2.8-3.5 ppm) without significantly changing the residual. This fit (Table 4 and Fig. 5) gives Al occupancies of  $g_1 = 0.30$ ,  $g_2 = 0.41$ , and  $g_3 = 0.30$  and a mean Al NNN of  $1.99 \pm 0.03$ . Thus, in both of the first two fits we obtained an Al distribution in which Al is ordered onto the T2 site, the same result as that for KAS3.

Finally, we attempted to fit the spectrum with a distribution similar to that proposed by Murdoch et al. (1988). The starting point for this was a T2 envelope with a shift 4.3 ppm per Al substitution, peak widths of 3 ppm, peak intensities in the ratio 1:2:4:2:1, and the T2 (2Al) peak at -91.6 ppm (the position of the central bump in the spectrum). All the parameters for the T1 and T3 peaks were then allowed to vary and the fit refined by fixing some of the small 4Al and 0Al peaks to give an internally consistent solution. This fitting strategy resulted in an equally small  $\chi^2$  and Al occupancies of around  $g_1 = 0.4$ ,  $g_2 = 0.2$ , and  $g_3 = 0.4$ , i.e., Al ordered onto T1 and T3.

In summary, the  $^{29}\text{Si}$  spectrum of KAS2 can be simulated adequately in many different ways, and at present it does not appear to be possible to make an unequivocal interpretation of the spectrum. However, we can at least say that the spectrum is consistent with the ordering scheme we have observed for the ordered analogue, KAS3. By analogy with KAS3 and using the principal of Oc-

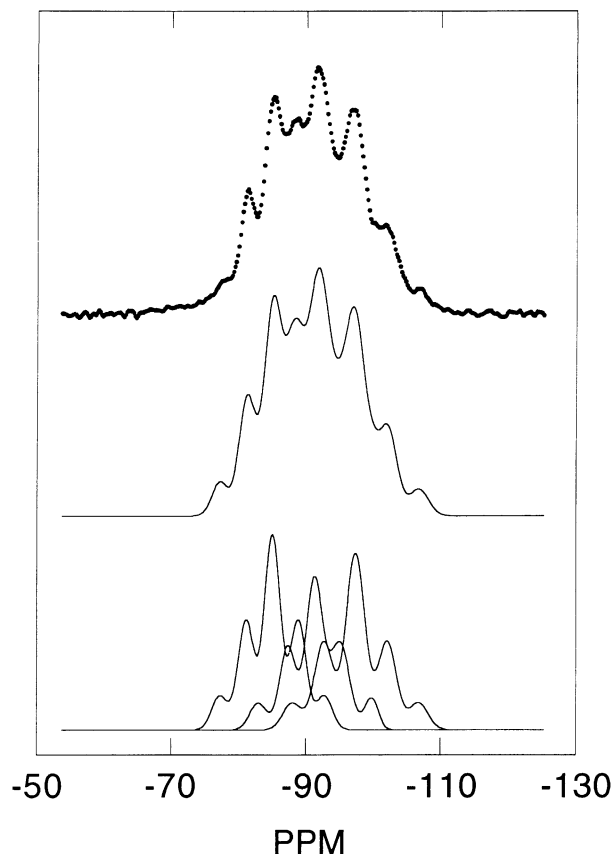


Fig. 5. A simulation of  $^{29}\text{Si}$  spectrum of Alban Hills leucite, KAS2, with an ordering scheme in which Al is ordered onto the T2 site. (upper) Experimental data. (middle) Simulation of spectrum with the 15 peaks listed in Table 4 (includes internal consistency constraint). (lower) The three sets of peaks for the three T sites.

cam's Razor that "multiplicity ought not to be advocated without necessity," we feel that Al ordering onto T2 is somewhat more probable than the alternatives. The implications of these findings to the previous studies of ordering in leucite will be discussed later.

The three  $^{27}\text{Al}$  peaks in the 14.1 T spectrum for the Alban Hills leucite (Fig. 4b) are less well resolved than those in the analcite-derived leucite and resemble the spectrum for the  $1/2$  to  $-1/2$  transition reported by Phillips et al. (1989). As with KAS3, it is possible to obtain what appears to be a reasonable fit using mixed Gaussian and Lorentzian lines, but the relative peak areas are in very poor agreement with the results of the simulation of the  $^{29}\text{Si}$  spectrum. Bearing in mind the difficulties in simulating the relatively well-resolved spectra for KAS3, it was not considered worthwhile to fit the spectra of KAS2 using quadrupolar lineshapes. As with KAS3, it appears that inadequate constraints on the  $^{27}\text{Al}$  lineshapes make it impossible to obtain meaningful independent site-occupancy data from the  $^{27}\text{Al}$  spectrum of the natural leucite.

TABLE 5. Summary of typical Al occupancies suggested by various studies

	Technique	$g_1$	$g_2$	$g_3$
Mazzi et al. (1976)	XRD	0.33	0.33	0.33
Brown et al. (1987)	NMR	0.56	0.36	0.08
Murdoch et al. (1988)	NMR	0.39	0.16	0.42
Phillips et al. (1989)	NMR	0.50	0.25	0.25
Boysen (1990)*	Neut. diff.	<0.33	>0.33	<0.33
Palmer (1990) (at 4 K)	Neut. diff.	0.18	0.43	0.39
KAS3 (this study)**	NMR	0.18	0.48	0.33
KAS3 (this study)†	NMR	0.27	0.47	0.27
KAS2 (this study)††	NMR	0.30	0.41	0.30

\* No ordering data were published.

\*\* Best numerical fit but without internal consistency.

† With internal consistency constraint.

†† This is simply an illustration that KAS2 can be fitted with these parameters. It is equally well fitted by a wide range of Al distributions.

The  $^{27}\text{Al}$  peak maxima are 0.5–1.2 ppm more positive for KAS2 than KAS3, whereas the  $Q^4(2\text{Al})$   $^{29}\text{Si}$  shifts are essentially the same for both samples. The explanation for this is not clear. However, it should be noted that Al has four Si NNN compared with an average of two Al NNN for each Si, i.e., they are not sampling the same distribution. In addition, the Al peak position is affected by the electric-field gradient as well as the isotropic chemical shift; both are affected by the T-O-T bond angle, and the broader  $^{29}\text{Si}$  lines indicate that there is a wider distribution of bond angles in KAS2 than KAS3. If the Al atoms that have smaller bond angles (and thus more positive shift) also have a smaller electric-field gradient, then the quadrupolar contribution to the shift and linewidth is less as well; conversely, if the Al atoms that have larger bond angles also have a larger electric-field gradient, then the peak shifts and broadens in a more positive direction. As a consequence the peak position may become slightly more positive even with similar mean bond angles.

In Table 5, we compare the mean Al occupancies of our two samples with the occupancies suggested by the three previous NMR studies (Brown et al., 1987; Murdoch et al., 1988; Phillips et al., 1989) and by neutron diffraction studies (Boysen, 1990; Palmer, 1990). Our results for the ordered leucite sample are consistent with the results of both neutron diffraction studies, but note that Boysen (1990) did not give estimates of the degree of ordering onto T2. The probable sources of error in the previous NMR studies are discussed in the following section.

#### DISCUSSION OF PREVIOUS NMR STUDIES

The positions of the peaks in the  $^{29}\text{Si}$  spectrum of the leucite derived by ion exchange imply that the assignment of the  $^{29}\text{Si}$  spectra of leucite suggested by Phillips et al. (1989) is incorrect. Because the peak at  $-97.0$  ppm is due mainly to  $Q^4(2\text{Al})$  Si in T1, the shoulder at  $-102$  ppm represents  $Q^4(1\text{Al})$  Si in T1, and the feature at  $-107$  ppm is due to  $Q^4(0\text{Al})$  Si in T1. The intensity at  $-111$  ppm (<3% of the total) observed by Phillips et al. (1989) therefore cannot be due to a distinct Si environment in

the leucite but could be due to some impurity phase at a level that is too low to be detected by XRD.

Furthermore, the problems we encountered in simulating the  $^{27}\text{Al}$  spectra, even for the leucite derived by ion exchange where the three peaks are relatively well resolved, also apply to the treatment of  $^{27}\text{Al}$  data by Phillips et al. (1989). The overall shape of the resonance of the  $^{27}\text{Al}$  center band in Phillips et al. (1989) bears some resemblance to ours in that it is skewed, giving the effect of having a tail with more negative shifts. To fit this tail, their fitting program is forced to make the T1 peak broad and to have a large Lorentzian component. As a result, the T2 peak is forced to be smaller than it should be, leading to erroneous conclusions. If the T2 peak is asymmetric (as discussed earlier) and extends to much less positive shifts than in the simulation of Phillips et al. (1989), the area of the T1 peak is forced to be smaller, and the area of the T2 peak is larger. The spectrum could then yield areas for the three peaks that are consistent with the Al-Si ordering suggested by the present study. Phillips et al. (1989) were in fact careful to point out the possible drawbacks in their  $^{27}\text{Al}$  simulations but chose symmetrical lineshapes in the absence of any additional information. In the light of our new data it appears that attempts to simulate  $^{27}\text{Al}$  MAS NMR spectra of leucite cannot currently give quantitative site-ordering information.

In the study of Murdoch et al. (1988), the  $^{29}\text{Si}$  spectrum of the natural leucite specimen is indistinguishable from that of our KAS2, and the assignments of the  $^{29}\text{Si}$  spectra are also essentially the same as those deduced in the present work. However, although they use a variety of carefully thought out, sophisticated fitting methods, the Si-Al occupancies they deduce are very different from those deduced here for the ordered leucite. In view of the wide range of possible solutions we have found for our natural leucite spectrum it appears that there are many possible minima in the parameter surface. The ordering scheme proposed by Murdoch et al. (1988) therefore is not unique. Models 1 and 2 of Murdoch et al. (1988) involve fitting eight peaks to the eight observable features in the  $^{29}\text{Si}$  spectrum, then assigning each of the 15 peaks that should be present to one of these eight features. The weakness of these models is that there is no reason to expect that unrelated peaks, such as  $Q^4(4\text{Al})$  on T1,  $Q^4(3\text{Al})$  on T2, and  $Q^4(2\text{Al})$  on T3, have the same chemical shift. Therefore, if this assumption is made, one cannot expect very reliable ordering data.

Model 3 of Murdoch et al. (1988) is related to the first method used here in that: (1) three sets of five peaks are used; (2) for each site the shift difference between each of the five peaks is set to be constant, i.e., for a given T site the effect of each Al substitution on the shift is constant, and (3) the width of all five peaks within each group is constant. However, it is possible to force fits to give a wide variety of different ordering patterns with equally good residuals.

The fact that four different NMR studies of leucite

(Brown et al., 1987; Murdoch et al., 1988; Phillips et al., 1989; this work) have produced four different Al-Si ordering schemes for leucite is very unsatisfactory. We therefore tried additional tests for the scheme of Murdoch et al. (1988) (Al ordering onto T1 and T3) and two versions of a scheme with Al ordering onto T2. The data were tested against the simulation of cubic  $\text{CsAlSi}_2\text{O}_6$  presented by Phillips and Kirkpatrick (1994) and our fit of a 500 °C spectrum of leucite, also presented by Phillips and Kirkpatrick (1994). Unfortunately, however, in both cases the spectra can be simulated equally well with the parameters proposed by Murdoch et al. (1988) or those presented in Tables 3 and 4.

We reexamined the original X-ray structural data of Mazzi et al. (1976), to look for any indirect evidence for Al ordering hidden in the bond angles and bond lengths. Hill and Gibbs (1979) performed linear regression analyses on structural data for the silica polymorphs and proposed the following correlation between the secant of the T-O-T angle and the Si-O bond length:

$$d_{(\text{Si-O})_{\text{br}}} = 1.526 - 0.068 \sec(\angle \text{Si-O-Si}). \quad (1)$$

Although the equivalent expression for framework aluminosilicates is not available, the major change in bond length with Al substitution is due to the increase in the constant term in Equation 1. Thus, by taking the T-O-T angles given by Mazzi et al. (1976) and using the mean of the secants of the four T-O-T angles for each tetrahedron, one can calculate the differences in the mean T-O bond lengths between the sites. This procedure predicts, for equal occupancy on each T site, that  $d_{\text{T1-O}}$  should be  $\sim 0.010$  Å shorter than  $d_{\text{T2-O}}$ , and that  $d_{\text{T3-O}}$  should be  $\sim 0.012$  Å longer than  $d_{\text{T2-O}}$ . In contrast, the mean Si-O bond lengths given by Mazzi et al. (1976) are 1.643, 1.656, and 1.656 Å for T1, T2, and T3 sites, respectively, i.e.,  $d_{\text{T1-O}}$  is 0.013 Å shorter than  $d_{\text{T2-O}}$  and  $d_{\text{T3-O}}$  is identical to  $d_{\text{T2-O}}$ . As the T-O bond length will clearly be larger if Al is substituted for Si, and the  $d_{\text{T2-O}}$  found by Mazzi et al. (1976) data appears to be too long, it can be argued that the T2 site contains relatively more Al than the T1 and T3 sites. Although this line of reasoning involves several assumptions and can be considered to be only secondary evidence, it is interesting that the original single-crystal X-ray diffraction data of Mazzi et al. (1976) are consistent with the proposal based on our NMR studies of a synthetic ordered leucite, i.e., that Al is ordered onto the T2 site.

Despite the problems encountered in this and earlier studies, NMR has a major role to play in improving our understanding of the structure and behavior of leucite. The mechanisms of the displacive tetragonal-cubic phase transition in leucite are still not fully understood, and there is still some uncertainty regarding whether or not any reversible change in Si-Al order occurs at elevated temperature, as the transition is approached. In natural leucite, the high-temperature tetragonal-cubic phase transition has been shown to occur in two stages:  $I4_1/a \rightarrow I4_1/acd$  and  $I4_1/acd \rightarrow Ia3d$  (Lange et al., 1986; Palmer

et al., 1989; Boysen, 1990) [it should be noted that not all workers agree with these space group assignments (Ito et al., 1991)]. At the  $I4_1/a \rightarrow I4_1/acd$  transition the T1 and T3 sites become identical, and at the  $I4_1/acd \rightarrow Ia3d$  transition all T sites become identical. It is generally believed that the timescale of Si-Al ordering in framework aluminosilicates is too slow for T-site ordering to occur during rapidly reversible phase transitions. In principle, the three distinct T sites in  $I4_1/a$  leucite could each have different Si-Al occupancies, but the transition to  $I4_1/acd$  should only occur for samples with identical ordering arrangements in T1 and T3. Thus, if the Al occupancies in natural leucites are close to 0.25 for T1 and T3 and 0.5 for T2, as observed for KAS3, then it is possible that at some elevated temperature T1 and T3 become equivalent, resulting in a three T-site to two T-site transition. Above this transition, there would be a site with Al occupancy of 0.25 and multiplicity of 2 and a site with Al occupancy of 0.5 and multiplicity of 1. This could possibly explain the  $I4_1/a$  to  $I4_1/acd$  transition. However, the  $I4_1/acd$  to  $Ia3d$  transition can be explained only by disorder of Si and Al over the T sites or by creation of some structure that is isotropic at the observational length scale of X-ray diffraction but contains domains of lower symmetry (i.e., the structure is not truly  $Ia3d$ ). The structural changes that occur on approaching the cubic-tetragonal transition are currently being investigated by (1) studying the Rb and Cs analogues of KAS3 and KAS2, which at room temperature are closer to the tetragonal-cubic transition temperatures (Kohn et al., in preparation), and (2) in-situ high-temperature  $^{29}\text{Si}$  MAS NMR experiments of these samples.

#### ACKNOWLEDGMENTS

We would like to thank D. Reed, A.P. Howes, and Z.P. Han for help with various aspects of the NMR experiments and simulations, NERC and SERC for financial support, and SERC for provision of the VXR 600 service. We are most grateful for the reviews of B.L. Phillips and J.F. Stebbins, which stimulated us into reconsidering some of our original conclusions.

#### REFERENCES CITED

- Boysen, H. (1990) Neutron scattering and phase transitions in leucite. In E.K.H. Salje, Ed., *Phase transitions in ferroelastic and coelastic crystals*, p. 334–349. Cambridge University Press, Cambridge, U.K.
- Brown, I.W.M., Cardile, C.M., MacKenzie, K.J.D., Ryan, M.J., and Meinhold, R.H. (1987) Natural and synthetic leucites studied by solid state  $^{29}\text{Si}$  and  $^{27}\text{Al}$  NMR and  $^{57}\text{Fe}$  Mössbauer spectroscopy. *Physics and Chemistry of Minerals*, 15, 78–83.
- Dove, M.T., Cool, T., Palmer, D.C., Putnis, A., Salje, E.K.H., and Winkler, B. (1993) On the role of Al-Si ordering in the cubic-tetragonal phase transition of leucite. *American Mineralogist*, 78, 486–492.
- Fyfe, C.A., Thomas, J.M., Klinowski, J., and Gobbi, G.C. (1983) Magic angle spinning NMR (MAS-NMR) spectroscopy and the structure of zeolites. *Angewandte Chemie International English Edition*, 22, 259–275.
- Hatch, D.M., Ghose, S., and Stokes, H.T. (1990) Phase transitions in leucite,  $\text{KAlSi}_3\text{O}_6$ : I. Symmetry analysis with order parameter treatment and the resulting microscopic distortions. *Physics and Chemistry of Minerals*, 17, 220–227.
- Hill, R.J., and Gibbs, G.V. (1979) Variation in  $d(\text{T-O})$ ,  $d(\text{T}\cdots\text{T})$  and  $\angle\text{TOT}$  in silica and silicate minerals, phosphates and aluminates. *Acta Crystallographica*, B35, 25–30.
- Hovis, G.L. (1986) Behavior of alkali feldspars: Crystallographic properties and characterization of composition and Al-Si distribution. *American Mineralogist*, 71, 869–890.
- Ito, Y., Kuehner, S., and Ghose, S. (1991) Phase transitions in leucite determined by high temperature single crystal X-ray diffraction. *Zeitschrift für Kristallographie*, 197, 75–84.
- Jäger, C., Rocha, J., and Klinowski, J. (1992) High-speed satellite transition  $^{27}\text{Al}$  MAS NMR spectroscopy. *Chemical Physics Letters*, 188, 208–212.
- Kirkpatrick, R.J. (1988) MAS NMR spectroscopy of minerals and glasses. In *Mineralogical Society of America Reviews in Mineralogy*, 18, 341–403.
- Kohn, S.C., Dupree, R., Mortuza, M.G., and Henderson, C.M.B. (1991) An NMR study of structure and ordering in synthetic  $\text{K}_2\text{MgSi}_3\text{O}_{12}$ , a leucite analogue. *Physics and Chemistry of Minerals*, 18, 144–152.
- Kohn, S.C., Henderson, C.M.B., and Dupree, R. (1994) NMR studies of the leucite analogues  $\text{X}_2\text{YSi}_3\text{O}_{12}$ , where X = K, Rb, Cs; Y = Mg, Zn, Cd. *Physics and Chemistry of Minerals*, 21, 176–190.
- Klinowski, J., Ramdas, S., and Thomas, J.M. (1982) A re-examination of Si, Al ordering in zeolites NaX and NaY. *Journal of the Chemical Society, Faraday Transactions*, 278, 1025–1050.
- Lange, R.A., Carmichael, I.S.E., and Stebbins, J.F. (1986) Phase transitions in leucite ( $\text{KAlSi}_3\text{O}_6$ ), orthorhombic  $\text{KAlSiO}_4$ , and their iron analogues ( $\text{KFeSi}_3\text{O}_6$ ,  $\text{KFeSiO}_4$ ). *American Mineralogist*, 71, 937–945.
- Mazzi, F., Galli, E., and Gottardi, G. (1976) The crystal structure of tetragonal leucite. *American Mineralogist*, 61, 108–115.
- Mazzi, F., and Galli, E. (1978) Is each analcime different? *American Mineralogist*, 63, 448–460.
- Murdoch, J.B., Stebbins, J.F., Carmichael, I.S.E., and Pines, A. (1988) A silicon-29 nuclear magnetic resonance study of silicon ordering in leucite and analcime. *Physics and Chemistry of Minerals*, 15, 370–382.
- Palmer, D.C. (1990) Phase transitions in leucite. Ph.D. thesis, University of Cambridge, Cambridge, U.K.
- Palmer, D.C., Salje, E.K.H., and Schmah, W.W. (1989) Phase transitions in leucite: X-ray diffraction studies. *Physics and Chemistry of Minerals*, 16, 714–719.
- Palmer, D.C., and Salje, E.K.H. (1990) Phase transitions in leucite: Dielectric properties and transition mechanism. *Physics and Chemistry of Minerals*, 17, 444–452.
- Peacor, D.R. (1968) A high temperature single crystal diffractometer study of leucite,  $(\text{K},\text{Na})\text{AlSi}_3\text{O}_6$ . *Zeitschrift für Kristallographie*, 127, 213–224.
- Phillips, B.L., and Kirkpatrick, R.J. (1994) Short-range Si-Al order in leucite and analcime: Determination of the configurational entropy from  $^{27}\text{Al}$  and variable-temperature  $^{29}\text{Si}$  NMR spectroscopy of leucite, its Cs- and Rb-exchanged derivatives, and analcime. *American Mineralogist*, 79, 1025–1031.
- Phillips, B.L., Kirkpatrick, R.J., and Hovis, G.L. (1988)  $^{27}\text{Al}$ ,  $^{29}\text{Si}$ , and  $^{23}\text{Na}$  MAS NMR study of an Al,Si ordered alkali feldspar solid solution series. *Physics and Chemistry of Minerals*, 16, 262–275.
- Phillips, B.L., Kirkpatrick, R.J., and Putnis, A. (1989) Si,Al ordering in leucite by high-resolution  $^{27}\text{Al}$  MAS NMR spectroscopy. *Physics and Chemistry of Minerals*, 16, 591–598.
- Ramdas, S., and Klinowski, J. (1984) A simple correlation between isotropic  $^{29}\text{Si}$  NMR chemical shifts and T-O-T angles in zeolite frameworks. *Nature*, 308, 521–523.
- Smith, M.E. (1993) Application of  $^{27}\text{Al}$  NMR techniques to structure determination in solids. *Applied Magnetic Resonance*, 4, 1–64.

MANUSCRIPT RECEIVED MARCH 23, 1994

MANUSCRIPT ACCEPTED APRIL 5, 1995